Interaction between Polyelectrolyte Brushes in Poor Solvents

Sanjay Misra* and Matthew Tirrell

Chemical Engineering and Materials Science Department, University of Minnesota, Minneapolis, Minnesota 55455-0132

Wayne Mattice

Institute of Polymer Science, University of Akron, Akron, Ohio 44325-3909

Received March 12, 1996; Revised Manuscript Received May 17, 1996[⊗]

ABSTRACT: This study examines the structure of planar polyelectrolyte brushes and the disjoining pressure between such brushes in a poor solvent. The self-consistent field theory is used in this work in contrast with the earlier studies that used a step-density model. We predict that upon the reduction in solvent quality the brush collapses continuously whereas the step-density model predicts a first-order collapse. In a sufficiently poor solvent the brush shows a discontinuous density profile: (i) between the grafting surface and the discontinuity the density is dominated by the solvent translational entropy and (ii) beyond the discontinuity the density is determined by the counterion translational entropy. The force−distance profiles are also always continuous unlike the prediction of the step-density model, which predicts discontinuous collapse under constant external pressure.

Introduction

Polymer brushes formed by uncharged polymers have been the subject of intense theoretical and experimental treatment in the last decade.[1] The attention has turned recently to polyelectrolyte brushes which have very rich underlying physics[2−17] and numerous technological applications, including control of colloid stability,[18] water and wastewater treatment,[19] membrane tailoring,[20] controlled drug delivery,[21] and increasing polymer−polymer miscibility.[22] In addition, water-soluble polymers (mostly polyelectrolytes), being environmentally friendly, are increasingly displacing neutral polymers soluble in organic solvents. Theoretical investigations of model systems like brushes provide a simple way to probe the essential physics of these interfacial system.

Polyelectrolyte brush refers to a layer formed by densely attaching charged high-polymer chains to a surface. In this work, we focus on the structure of polyelectrolyte brushes and the interactions between such brushes in poor solvents. The poor solvent case is relevant because most polyelectrolyte chains have carbon backbones that are insoluble in water and the chains are solvated essentially by electrostatic interactions. This leads to some interesting phase behavior that has been explored by Zhulina and co-workers[8] and Ross and Pincus[9] using the Alexander−de Gennes[23,24] model which envisages a uniform polymer density in the brush. Henceforth we refer to it as the step-density model. Using the step-density model these works predict overall properties of polyelectrolyte brushes (thickness and average segment density). They also predict a discontinuous change in the brush thickness with solvent quality and a discontinuous change in thickness when such brushes are compressed.

The structure of the polyelectrolyte brush (i.e., segment density distribution) in good solvents has been studied using self-consistent field theory (SCF)[2−4,6,11] and by computer enumeration of polyelectrolyte chain conformations.[17] The polyelectrolyte brush structure in poor solvents however remains unexplored. We have recently shown that planar (as well as convex) polyelectrolyte brushes can have a two-phased structure in poor solvents.[16] Near the grafting surface the polymer density is high (dense phase dominated by ternary and higher order interactions) and changes discontinuously to a lower density (dilute phase dominated by electrostatic repulsion) as one moves away from the surface.

In what follows, we shall apply the self-consistent field theory to polyelectrolyte brushes in poor solvents. Our focus will be on elucidating the nature of the collapse of such brushes as the solvent quality becomes poorer and on the disjoining pressure between such brushes. The rest of the paper is organized as follows. The next section discusses the equation used for the free energy density and the consequences for the phase behavior of the brushes. In section 3 the SCF theory is outlined, with a view to determining the segment density distribution within the brush as well as the pressure profiles for compressed brushes. Section 4 deals with the results of the SCF theory. We examine the segment density distributions in free (uncompressed) and compressed brushes. A threshold density is defined below which a free brush is single-phased (dilute) and above which the brush has both the dense and dilute phases. The pressure between two compressed brushes is calculated from the SCF theory and compared with the step-density model. We conclude by highlighting the salient results of the SCF model for polyelectrolyte brushes in poor solvents.

Free Energy Density and Chemical Potential

Chemical Potential and the Phase Diagram. The equation of state used in this work is the same as that used by Pincus and Ross,[9] Borisov and co-workers,[8] and Misra et al.[16] Specifically, we assume that the brush is locally electroneutral, a condition that represents the physics more accurately as the brushes become more dense and as they come under compression. The added advantage, in adopting this approximation, is that the physics is simplified and comparison with the step-density models is facilitated. The local density of the counterions is the same as that of the dissociated polymer segments and, since the electric field uniformly vanishes, the term due to electrostatic stress drops out. The local free energy density and the local chemical potential (to within a constant) in the brush are given

* E-mail: smisra@cems.umn.edu.

[⊗] Abstract published in *Advance ACS Abstracts,* July 15, 1996.

S0024-9297(96)00377-4 CCC: $12.00 © 1996 American Chemical Society

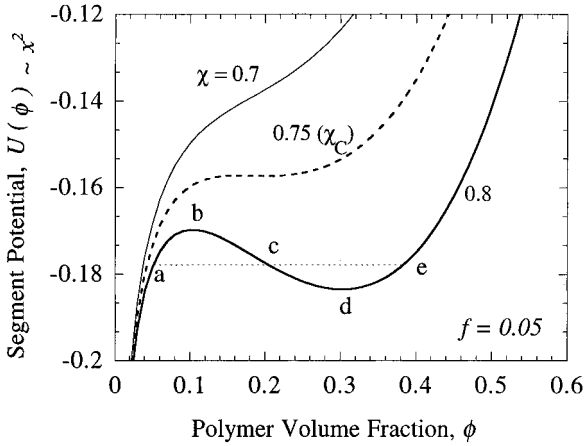

Figure 1. Chemical potential (eq 2) of a polymer segment as a function of the polymer volume fraction. When $\chi > \chi_C$, the potential is two-valued and we have a phase separation with two phases in equilibrium. In order to obtain the densities of the two phases, we do a Maxwell equal-area construction, such that area(abca) = area(cdec).

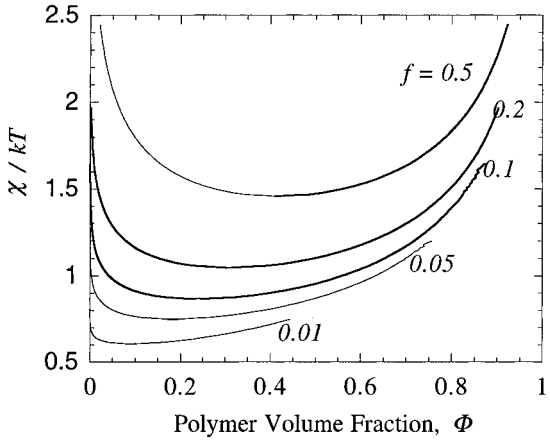

Figure 2. Phase diagram obtained from eq 1. The two-phase region shifts to higher values of χ as the charge fraction, f, increases; it also becomes more symmetric.

as

$$F(\phi) = (1 - \phi)\ln(1 - \phi) + \chi\phi(1 - \phi) + f\phi\ln(f\phi) \quad (1)$$

$$U(\phi) = \frac{\partial}{\partial\phi}F(\phi) = -\ln(1 - \phi) - 2\chi\phi + f\ln\phi \quad (2)$$

Here ϕ is the local polymer volume fraction, f is the fraction of polymer segments that are dissociated, and χ is the Flory−Huggins parameter. Equation 1 can also be looked at as the free energy density of a polyelectrolyte solution with infinitely long chains. For a given value of f there is a value of $\chi(\chi_C)$ at which the polyelectrolyte brush can phase separate. χ_C is determined by the conditions that

$$\frac{\partial}{\partial\phi}U(\phi) = 0 \quad (3)$$

$$\frac{\partial^2}{\partial\phi^2}U(\phi) = 0 \quad (4)$$

It can be shown that χ_C satisfies the following equation:

$$\chi_C = \frac{(1 - 2\chi_C - f)^2}{8f} \quad (5)$$

When $\chi < \chi_C$ the function $U(\phi)$ is single-valued, and when $\chi > \chi_C$ it is two-valued (showing an inflection point when $\chi = \chi_C$). The density of the two phases in equilibrium is determined by the Maxwell equal-area construction (see Figure 1), noting that U and ϕ are the conjugate variables. Figure 2 shows the phase diagram obtained using eq 1 for the free energy density. As expected, the value of χ_C increases as f increases and, in addition, the phase diagram becomes more symmetric.

We should expect that as the solvent quality is lowered below the value of χ_C or when the brush is compressed in a poor solvent, it would go from a single-phase brush to a brush in which the density changes discontinuously (from ϕ_L to ϕ_U). As mentioned in a previous work this situation is analogous to the collapse of a brush by *n*-clusters (a concept proposed by de Gennes for aqueous, uncharged polymer solutions).[25,26]

SCF Theory for Polyelectrolyte Brushes

We do not delve into the background of the self-consistent field theory in much detail; this has been discussed in detail in many prior publications (see for example refs 27−29). Milner, Witten, and Cates[28] have shown that for strongly stretched chains the polymer conformations are analogous to the trajectories of Newtonian particles. Assuming that the chains are monodisperse and that the chain ends are under no tension, the analogy reduces to that of Newtonian particles falling in an equal-time potential—the harmonic potential. The major conclusion of the SCF analysis is that the chemical potential of the polymer segments varies parabolically as a function of the distance from the grafting surface.[28]

$$U(\phi) = A - Bx^2 = -\ln(1 - \phi) - 2\chi\phi + f\ln\phi \quad (6)$$

Here A is a constant that depends upon the grafting density σ. B is another constant that equals (π^2/8), and x is the distance from the surface scaled by the chain length N. The value of A is fixed using the following mass balance:

$$\sigma = \int_0^L \phi\, dx \quad (7)$$

Note that $U \sim x^2$ and that U and ϕ are conjugate variables. The Maxwell equal-area construction can also be performed by plotting ϕ vs x^2; indeed this method has been used by Wagner et al. in the study of brush collapse by *n*-clusters and is also used in this study.

The calculations were performed by varying surface concentration of the polymer and plugging the resultant density profiles into eq 7 until the mass balance was satisfied. Equal-area construction was used to determine the density discontinuity whenever $\chi > \chi_C$.

Pressure Profiles. When two brushes are compressed against one another, they do so without any significant interpenetration. There is no force on the midplane arising from chain tension since no chains cross the midplane. The chain ends that contact the midplane do not exert any force since they are randomly oriented. The only force at the midplane, as pointed out by Milner et al.,[28] is the local osmotic pressure. At equilibrium this is balanced by an external force. Assuming that the thickness of the compressed brush is L, the external pressure needed to achieve this compression is given by

$$P = \Pi_L \quad (8)$$

where Π_L is the osmotic pressure evaluated at the

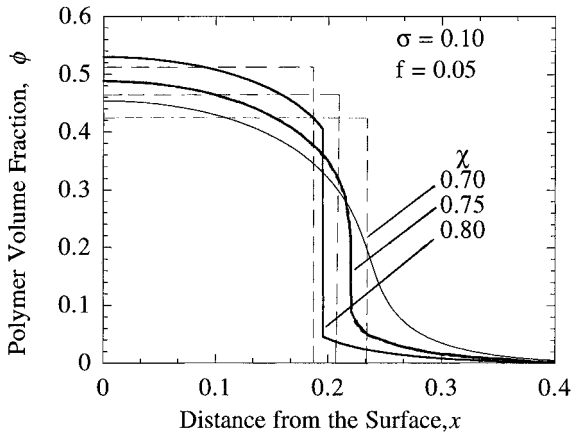

Figure 3. Segment density profiles using the SCF theory for different solvent qualities. In good solvents the density profile is continuous, whereas in poor solvents the density changes discontinuously ($\chi_C = 0.75$). The corresponding density profiles, using the step-density model, are also shown.

midplane. The local osmotic pressure is given as

$$\Pi = \phi\frac{\partial}{\partial\phi}F(\phi) - F(\phi) = -\ln(1-\phi) - \chi\phi^2 - (1-f)\phi \tag{9}$$

For an equilibrium brush (no external forces) the proper boundary condition at the brush edge is $\Pi_L = 0$. Under good solvent conditions, this translates to $\phi = 0$ at the brush edge.

Step-Density Model. The results from the SCF model will be compared with the step-density model used by Pincus and Ross[9] and Borisov and co-workers.[8] To facilitate the comparison, we present the salient results of the step-density model below. The basic idea is to balance the osmotic pressure against the tension in the chains in the brush (it can be shown that this is equivalent to minimizing the brush free energy). In a step-density brush of thickness L, the polymer density is given as $\phi = (\sigma/L)$. The tension transmitted by the chains per unit area of the brush is $\sigma L = \sigma^2/\phi$. The difference between the tension and the osmotic pressure is the external pressure

$$P = \Pi - T = -\ln(1-\phi) - \chi\phi^2 - (1-f)\phi - \frac{\sigma^2}{\phi} \tag{10}$$

The equilibrium thickness is determined by setting $P = 0$. As we show later, in poor solvents ($\chi > \chi_C$), the P vs L diagram resembles the $P-V$ diagram of a van der Waals gas.[9] One needs to do an equal-area construction on a plot of P vs L in order to determine the disjoining pressure at which the thickness changes discontinuously. Discontinuous thickness change at zero disjoining pressure points to a first-order collapse of the polyelectrolyte brush.[8,9]

Density Profiles and Pressure Profiles

Segment Density Profiles. In Figure 3 we show some typical density profiles (for uncompressed brushes) as χ is changed, keeping fixed σ (0.01) and f (0.05). Step-density profiles corresponding to these parameters are also shown. The density profile is continuous when $\chi \le \chi_C(0.75)$ and becomes discontinuous when $\chi > \chi_C$. At $\chi = \chi_C$, the density profile shows an inflection. When χ is sufficiently above χ_C, then the density profile has the following functional forms near the surface (dense phase) and far from the surface (dilute phase). Near the surface the translational entropy of the solvent dominates the segment potential and

$$\phi = 1 - \exp(-A + Bx^2), \qquad \phi > \phi_U \text{ (dense phase)} \tag{11}$$

The change in density with distance is small in this dense region. The average density in the dense region is approximately $|1 - 2\chi|$. Away from the surface, at lower densities, the translational entropy of the counterions dominates and

$$\phi = \exp\left(\frac{A - Bx^2}{f}\right), \qquad \phi < \phi_L \text{ (dilute phase)} \tag{12}$$

The density drops very rapidly in this dilute region. We must note here that the osmotic pressure at the edge of the brush vanishes only when the segment density vanishes. According to eq 12 therefore the brush thickness is infinite. This situation arises because of two reasons: (1) the brush is not actually electroneutral and the resultant term from the electric field is not accounted for and (2) the assumption that the chains are Gaussian allows the chains to be stretched far beyond their contour length. Nevertheless this does not pose a major problem since the segment density nearly vanishes well before the brush thickness reaches the contour length of the chains. Thus force−distance profiles predicted below do not show any significant repulsion until the brushes are compressed well below the contour length of the chains.

Note also that changing the solvent quality causes the the density profiles to shift in a continuous manner. The collapse of the brush upon reduction in solvent quality must also be continuous.

Threshold Grafting Density for a Two-Phase Brush. It should be noted that even when $\chi > \chi_C$ the segment density profile may not show a discontinuity if the grafting density is lower than a certain threshold. If the grafting density is below a certain threshold, σ_t, the surface concentration will be below ϕ_L, and therefore the brush will be a dilute, single-phase brush whose density is dominated by the counterion translational entropy (eq 12). If we assume that $\phi(x=0) \le \phi_L$ and use eq 12 for the segment density profile, we can show that

$$\sigma_t = \left(\frac{2}{\pi}\right)^{1/2}\phi_L f^{1/2} \tag{13}$$

σ_t is a function of χ and f only (since $\phi_L = \phi_L(\chi,f)$). Figure 4 shows the dependence of σ_t on χ for various values of f, using eq 13. σ_t drops sharply as χ increases; the decrease fits an exponential function very well as we move deeper into the two-phase region (i.e., with increasing χ). The line terminates at χ_C.

Pressure Profiles. Figure 5 shows some typical pressure−distance profiles for compressed brushes. Three broad features are noticeable. During the initial stage of compression, the applied pressure increases rapidly, dominated by the translational entropy of the counterions. As the brush gets compressed (and the density increases), the repulsive counterion pressure has to compete with the attractive binary interactions (since $\chi_C > \chi$). In this intermediate stage of compression, the brush thickness changes rapidly (but not discontinuously) with little change in the applied pressure. Finally, as the brush is compressed further, the density approaches its saturation value and the applied pressure increases rapidly again.

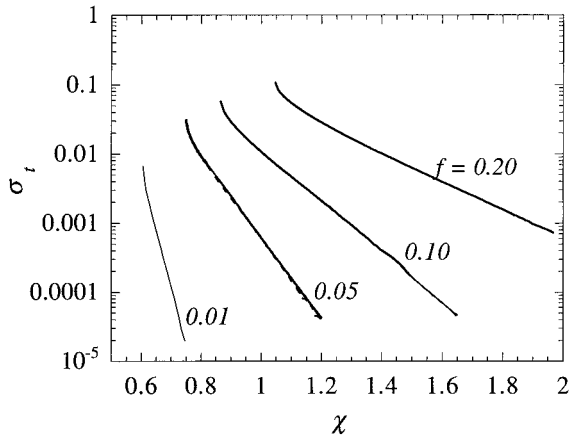

Figure 4. Threshold grafting density, σ_t, for realizing a two-phase brush as a function of χ. The decrease in the threshold grafting density is well approximated by an exponential function.

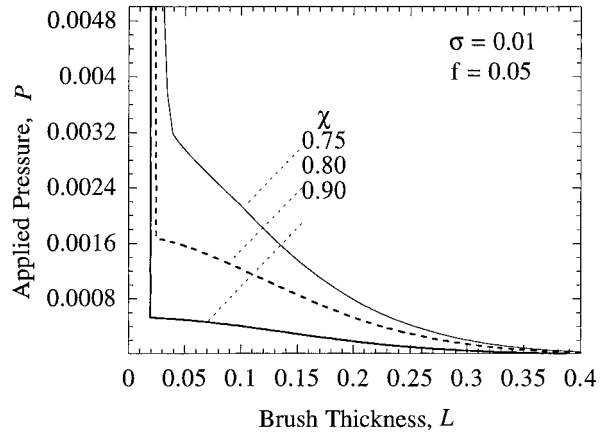

Figure 5. Applied pressure profiles for various values of χ, obtained from the SCF theory. For small compressions the counterion pressure dominates and the repulsion rises relatively fast. Further compression leads to a larger change in the thickness with smaller change in the pressure since attractive binary interaction competes with the counterion pressure. (The pressure is in units of kT/a^3, where a is the segment size.)

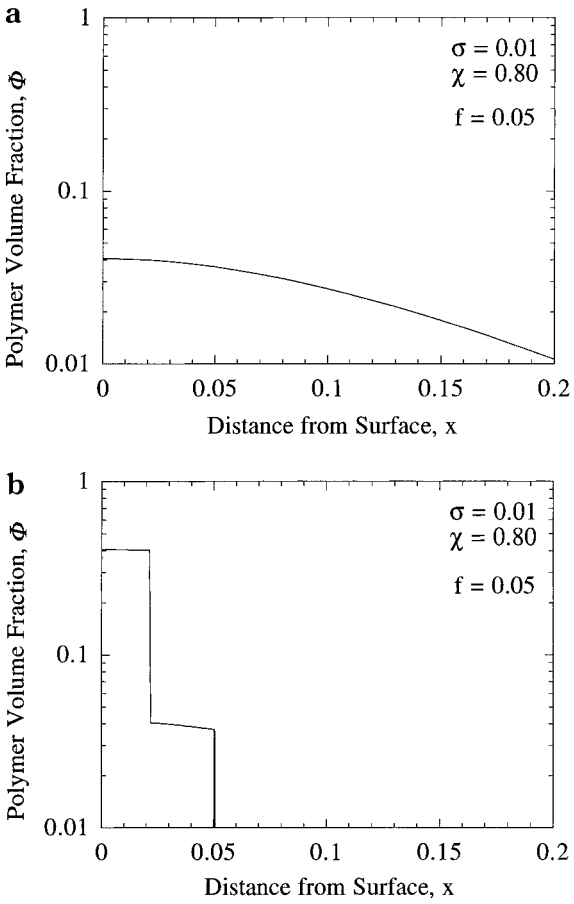

Figure 6. (a) Segment density profile for an uncompressed brush. For the given conditions the brush is a dilute single-phased brush. (b) Segment density profile for the compressed brush, under the same conditions. Upon compression the brush becomes two-phased.

Figures 6a and 6b show density profiles corresponding to a brush under different stages of compression. The uncompressed brush is essentially a single-phase dilute brush. Under compression, with increasing density the brush becomes two-phased. If the brush is again decompressed, the dense phase may not "spring" back immediately. This is because there is an energy barrier to the density changing from dense to dilute. Note that in the dense region the intersegmental interaction is repulsive (three body), in the intermediate density it is attractive (negative excluded volume or binary interactions), and in the dilute regime the intersegmental interaction is again repulsive (electrostatic). As a two-phase compressed brush undergoes decompression the density in the dense region has to go through the intermediate (attractive intersegmental interactions) region before the electrostatically stabilized lower density is obtained. This process (dense → intermediate) is energetically unfavorable and represents an energy barrier that needs to be surmounted before the brush regains its equilibrium (dilute) density. Thus compression and decompression pressure profiles may show hysteresis when the experiment is performed on time scales shorter than the rearrangement time of the brush. Some recent surface force experiments by Watanabe et al. on interactions between polyelectrolyte brushes indeed show this kind of behavior.[30] The applied pressure during first compression is usually higher than that obtained under subsequent compression, indicating a rearrangement of the brush on compression which does not recover upon decompression. It is possible that a partial collapse of the brush into a two-phased structure, as shown by the theoretical model, may be responsible.

In Figure 7a we show a typical pressure profile obtained form the SCF theory with the corresponding profile from the step-density model. The main features that distinguish the two are (i) the SCF theory predicts repulsion at a longer range, (ii) the repulsion is "softer" for the SCF theory compared to the step-density theory, (iii) the step-density brush collapses discontinuously at a constant disjoining pressure whereas the SCF theory predicts a continuous collapse, and (iv) the two profiles are in closer agreement at higher compression where the density at the edge of the SCF brush is closer to the average density. While the SCF theory predicts a continuous collapse, we note that the collapse occurs with a smaller change in disjoining pressure as the solvent quality becomes poorer. Therefore for very poor solvents, even according to the SCF theory, the collapse may *appear* discontinuous.

In very poor solvents, however, the step-density model predicts that the brush is completely collapsed. Thus the range of repulsion is much shorter and the repulsion much stronger when one compares it with the SCF theory. A typical case is shown in Figure 7b.

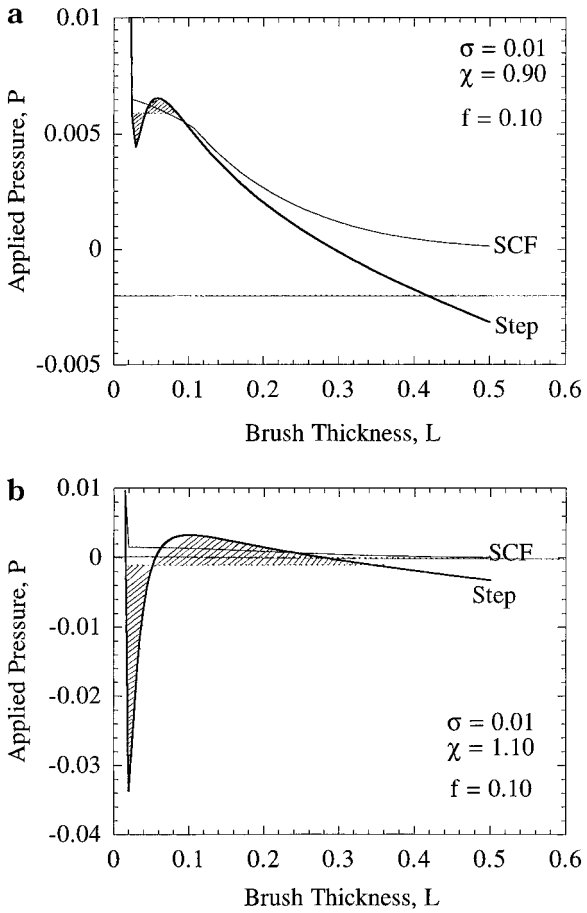

Figure 7. (a) Comparison of the applied pressure profiles obtained from the SCF theory and the step-density theory. The profile from the step-density theory is shorter ranged and steeper and shows a discontinuous collapse. (b) Comparison of the pressure profiles in very poor solvents. The step-density model predicts a collapsed brush under these conditions and consequently predicts a repulsion that is very shorter ranged and much steeper.

Conclusions

In this study we use the SCF theory to elucidate the structure of polyelectrolyte brushes in poor solvents as well as the interactions between such brushes. In poor solvents ($\chi > \chi_C$) the polyelectrolyte brush can be two-phased (if the grafting density is above a threshold grafting density). The polymer density changes discontinuously between a dense region adjoining the grafting surface and a dilute outer region. The brush collapses continuously as the solvent quality becomes poorer, in contrast to the step-density theory. Upon small compression, the disjoining pressure, dominated by counterion pressure, increases rapidly. When compressed further, the repulsion becomes much softer as attractive binary interactions compete with the counterion pressure. The repulsion predicted by the SCF theory is longer ranged and softer than that predicted by the step-density theory at all compressions. According to the SCF theory, the brush collapses continuously upon compression, whereas the step-density brush collapses discontinuously. In poorer solvents the change in thickness occurs with smaller change in the disjoining pressure and the collapse may appear to be discontinuous.

This work is based upon the mean field approximation where density in the lateral direction is assumed to be smeared out. It is possible, under certain conditions, that density fluctuations in the lateral direction, in poor solvents, could become important. Mesophase separation in bulk solutions has been predicted by Borue and Erukhimovich,[31] but whether these mesophases are observed in brushes would depend upon many factors including the thickness of the brush and the fact that the chains are tethered at the surface. These issues would require a more detailed examination along the lines of the work on uncharged polymer brushes by Ross and Pincus[32] and Yeung et al.[33]

Acknowledgment. We are grateful for support of research in this area by the National Science Foundation (Grant NSF/CTS 9107025, CTS and DMR Divisions) and by the CIE, an NSF Engineering Research Center at the University of Minnesota.

References and Notes

(1) Halperin, A.; Tirrell, M.; Lodge, T. P. *Adv. Polym. Sci.* **1992**, *100*, 31.
(2) Miklavic, S. J.; Marcelja, S. *J. Phys. Chem.* **1988**, *92*, 6718.
(3) Misra, S.; Varanasi, S.; Varanasi, P. P. *Macromolecules* **1989**, *22*, 4173.
(4) Misra, S.; Varanasi, S. *Macromolecules* **1991**, *24*, 322.
(5) Pincus, P. *Macromolecules* **1991**, *24*, 2912.
(6) Misra, S.; Varanasi, S. *J. Chem. Phys.* **1991**, *95*, 2183.
(7) Zhulina, E. B.; Borisov, O. V.; Pryamitsyn, V. A.; Birshtein, T. M. *Macromolecules* **1991**, *24*, 140.
(8) Borisov, O. V.; Birshtein, T. M.; Zhulina, E. B. *J. Phys. II* **1991**, *1*, 521.
(9) Ross, R.; Pincus, P. *Macromolecules* **1992**, *25*, 2177.
(10) Argillier, J. F.; Tirrell, M. *Theor. Chim. Acta* **1992**, *82*, 343.
(11) Zhulina, E. B.; Borisov, O. V.; Birshtein, T. M. *J. Phys. II* **1992**, *2*, 63.
(12) Misra, S.; Varanasi, S. *Macromolecules* **1993**, *26*, 4184.
(13) Zhulina, E. B. *Macromolecules* **1993**, *26*, 6273.
(14) Wittmer, J.; Joanny, J. F. *Macromolecules* **1993**, *26*, 2691.
(15) Dan, N.; Tirrell, M. *Macromolecules* **1993**, *26*, 4310.
(16) Misra, S.; Mattice, W. L.; Napper, D. H. *Macromolecules* **1994**, *27*, 7090.
(17) Von Goeler, F.; Muthukumar, M. *Macromolcules* **1995**, *28*, 6608.
(18) Napper, D. H. *Polymeric Stabilization of Colloidal Dispersions*; Academic: London, 1983.
(19) Schwoyer, W. L. K., Ed. *Polyelectrolytes for Water and Wastewater Treatment*; CRC Press: Boca Raton, FL, 1981.
(20) Saito, K.; Ito, M.; Yamagishi, H.; Furusaki S.; Sugo, T.; Okamoto, J. *Ind. Eng. Chem. Res.* **1989**, *28*, 1808.
(21) *NAMS Membr. Q.* **1990**, *5*, 2.
(22) Khokhlov, A.; Nyrkova, I. *Macromolecules* **1992**, *25*, 1493.
(23) Alexander, S. *J. Phys.* **1977**, *38*, 983.
(24) de Gennes, P.-G. *Adv. Colloid Interface Sci.* **1987**, *27*, 189.
(25) de Gennes, P.-G. *C. R. Acad. Sci. Paris II* **1991**, *313*, 1117.
(26) Wagner, M.; Brochard-Wyart, F.; Hervet, H.; de Gennes, P.-G. *Colloid Polym. Sci.* **1993**, *271*, 621.
(27) Semenov, A. N. *Sov. Phys.—JETP (Engl. Transl.)* **1985**, *61*, 733.
(28) Milner, S. T.; Witten, T. A.; Cates, M. E. *Macromolecules* **1988**, *21*, 2610.
(29) Skvortsov, A. M.; Gorbunov, A. A.; Pavlushkov, I. E.; Zhulina, E. B.; Borisov, O. V.; Priamitsyn, V. A. *Polym. Sci. USSR (Engl. Transl.)* **1988**, *30*, 1706.
(30) Watanabe, H.; Patel, S. S.; Argillier, J. F.; Parsonage, E. E.; Mays, J.; Dan-Brandon, N.; Tirrell, M. *Mater. Res. Soc. Symp. Proc.* **1992**, *249*, 255.
(31) Borue, V. Yu.; Erukhimovich, I. Ya. *Macromolcules* **1988**, *21*, 3240.
(32) Ross, R.; Pincus, P. *Europhys. Lett.* **1992**, *19*, 79.
(33) Yeung, C.; Balazs, A. C.; Jasnow, D. *Macromolecules* **1993**, *26*, 1914.

MA960377I